TOMOGRAPHIC RECONSTRUCTION CAMERA

Clarifying and visualizing sources of x-radiation using circular penumbra analysis

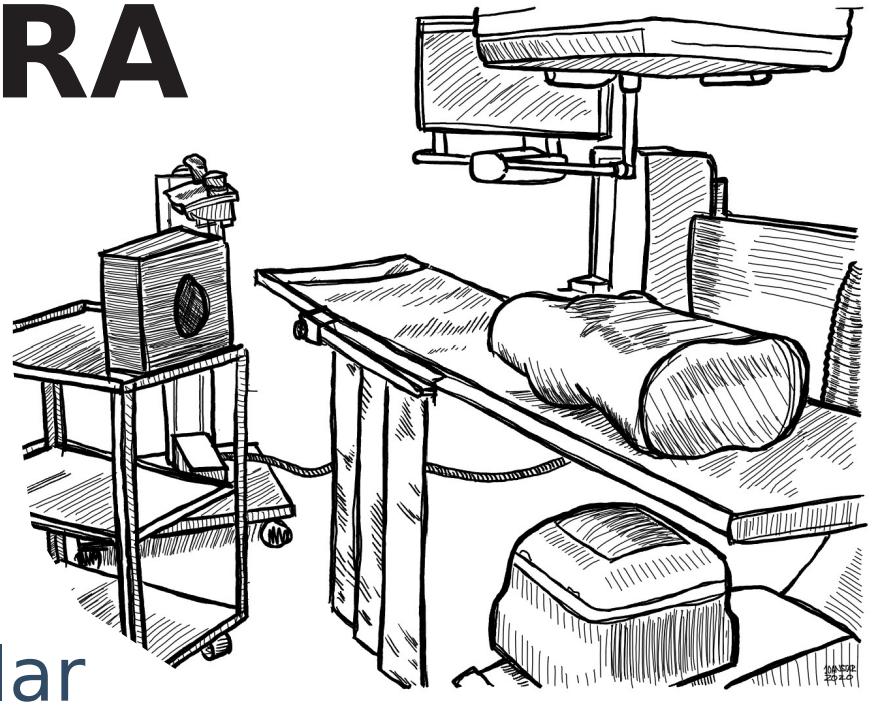

X-ray scatter sources can be imaged using a new type of camera called a Tomographic Reconstruction (TR) Camera. Visualizing x-ray scatter will allow identification of scatter sources and help inform medical staff to minimize their exposure to x-radiation.

Joan Brewer[1], Reece Walsh[1], Andrew Nicholson[1], Jonathan F. Holzman[1], Thorarin Bjarnason[1,2,3]

[1]University of British Columbia, Kelowna, Canada, [2]University of British Columbia, Vancouver, Canada, [3]Interior Health, Kelowna, Canada

ABSTRACT

Purpose: To visualize x-ray scatter using the novel tomographic reconstruction (TR) camera based on circular penumbra analysis; to produce these visualizations at clinical x-ray doses.

Methods: The TR camera was constructed as a box made of 4.76 mm steel, with a hole several centimetres in diameter cut in the front to serve as the aperture. A CR plate was placed in the back of the camera, at an adjustable depth ranging from 1.5 to 5 cm. The camera was exposed to four point sources using a radiographic tube, with a different number of exposures at each point to produce differing relative intensities (at a distance of 300 cm with73 kVp and 0.4 mAs per exposure). Reconstruction of the point sources served as proof of concept. Later, the camera was exposed to x-ray scatter using a fluoroscopy system with a torso phantom (at a distance of 1 m, with the system run until a DAP of 344 µGym2 was reached). A pinhole camera was constructed similarly to the TR camera (with a 3 mm diameter aperture), and was also exposed to the x-ray scatter. For the TR camera, both the point sources and scatter sources produced raw CR data which appeared as circular penumbra images; these data were used to reconstruct images of the sources. The TR camera x-ray scatter reconstructions were overlaid with photographs taken from the point of view of the TR camera, to visualize the sources.

Results: Faithful reproductions of x-ray point sources and x-ray scatter were produced using the TR camera (including accurate relative intensities), and the scatter sources were visualized by overlaying them with photographs. In order to collect x-ray scatter data using the pinhole camera, the fluoroscopy system had to be run until it reached a DAP eight times greater than was required by the TR camera.

Conclusions: This work shows that circular penumbra TR can be used to accurately visualize both x-ray point sources and x-ray scatter, and that reconstructions of x-ray scatter can be scaled to match photographs in order to visualize the sources.

Abbreviations: TR – tomographic reconstruction, CPA – circular penumbra analysis, CR – computed radiography, FBP – filtered back projection, FFT – fast Fourier transform, IR – iterative reconstruction, ART – algebraic reconstruction technique, MSE – mean square error, FOV – field of view

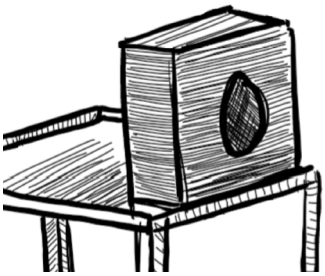

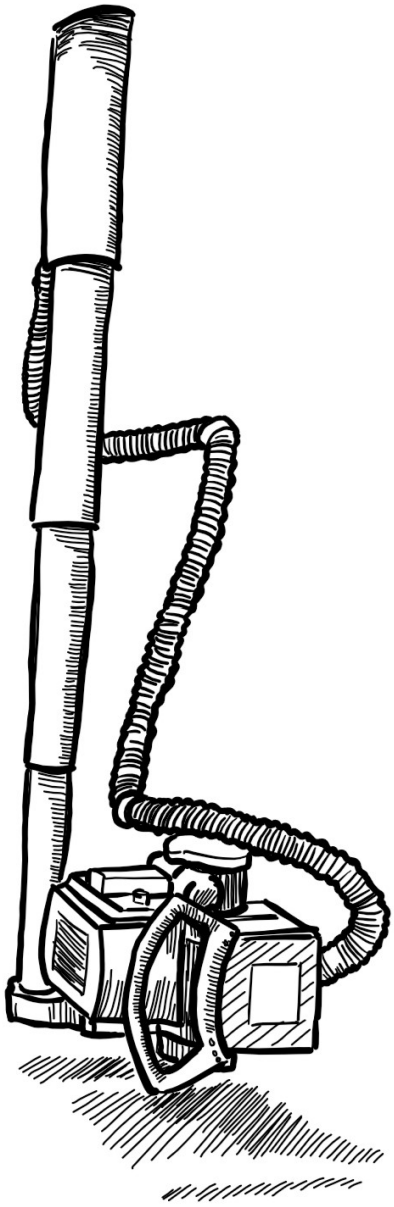

1. BACKGROUND

Systems such as x-ray machines and CT scanners, which are ubiquitous in healthcare settings and paramount in diagnostics, pose a workplace hazard to medical staff whom they continuously expose to low-dose x-ray radiation in the form of x-ray scatter. Protective measures such as lead-lined windows and lead aprons are used to attenuate x-rays reaching staff and minimize their exposure. In order to use these protective tools most effectively, knowledge of how x-rays scatter around different environments is required. This knowledge can be gained by imaging the x-ray scatter.

In an effort to do just that, Chida et al. proposed a method using a pinhole camera which contained an x-ray imaging plate overlaid with photographic film [Chida 2011]. This approach allowed for identification of sources of x-ray scatter within a given scene. However, due to its small aperture (on the order of 3 mm diameter), a pinhole camera requires a relatively high dose in order to produce an image. While high-dose situations allow for numerous x-rays to enter the camera and reach the detector, low-dose medical imaging techniques (such as fluoroscopy) would be unable to leverage Chida's technique during clinical operations due to insufficient exposure of the detector (resulting in noisy or non-existent images of the scatter).

A more common application of an x-ray pinhole camera is to measure the focal spot size of clinical radiology systems [Russo 2011], which is done routinely in order to maintain the quality of the systems [Di Domenico 2016]. In 2016, Di Domenico et al. proposed a new method of focal spot size measurement, called circular penumbra analysis (CPA), which involves tomographically reconstructing an image of the focal spot.

This work proposed to use an adjusted version of Chida's experimental setup whilst applying CPA to tomographically reconstruct images of x-ray scatter. This experiment required the design and manufacture of a new type of camera, called a tomographic reconstruction (TR) camera, which had a much larger aperture than a pinhole camera, enabling adequate exposure of the detector in low-dose scenarios.

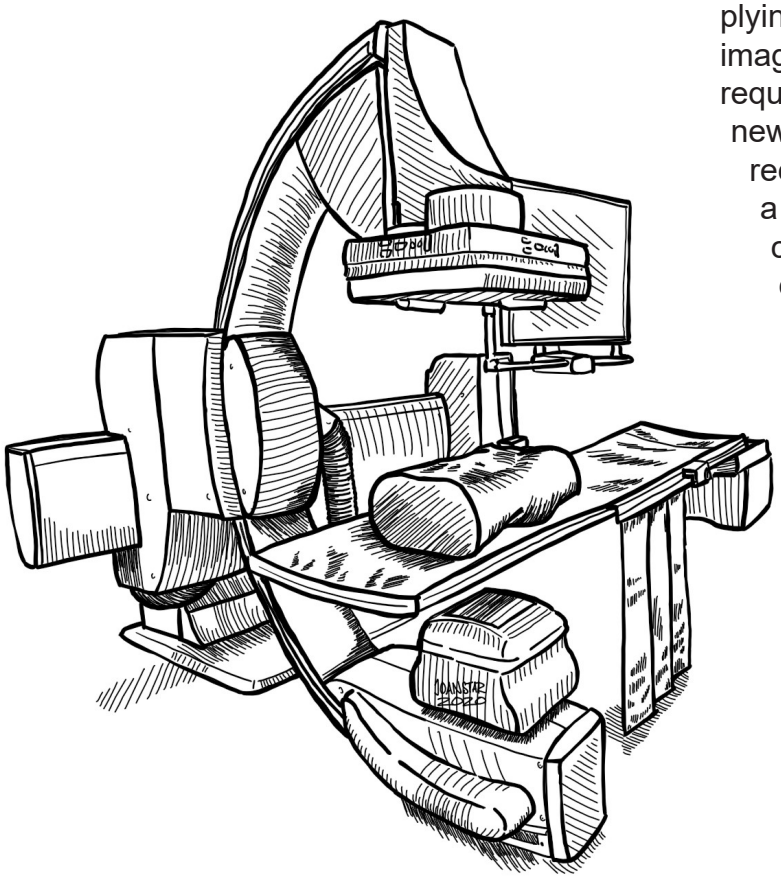

2. CIRCULAR PENUMBRA ANALYSIS
2.1 General Process

The setup for collecting data for CPA can be described as three separate, parallel planes (figure 1). The first is the source plane, which is the location of the x-ray source (the surface off of which the x-rays are reflecting). The second plane is the disk; in the case of the TR camera the disk functions as the aperture. The third plane is the x-ray detector.

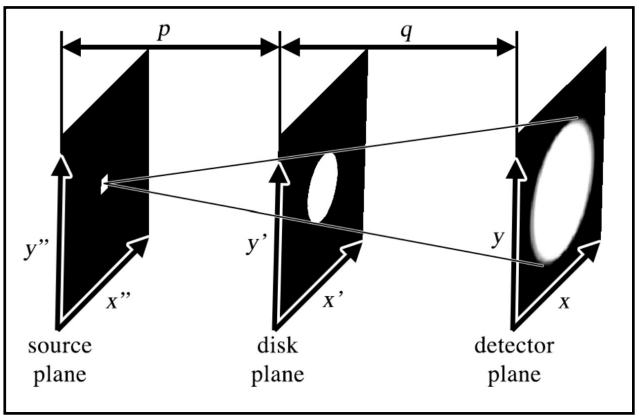

Figure 1. A diagram of the data collection setup, in which the source is projected through the disk plane onto a detector.

Briefly, the analysis process is made up of the following steps (through the use of a computer algorithm designed for this experiment):
1. The source (figure 2.a)) is projected through the disk onto the detector. This work used an 18 cm x 24 cm Fuji CR plate with 10 pixels per mm.
2. The detector is scanned. The raw data appears as a circular penumbra image. See figure 2.b).
3. The penumbra image is divided radially into n slices, often 360 or 720 slices depending on the image size. See figure 2.c).
4. The slices are aligned horizontally, giving a rectangular image. The image is manually cropped so that unnecessary pixels are eliminated and the sinogram is centred. See figure 2.d).
5. The derivative of the rectangular image is taken to produce a sinogram. See figure 2.e).
6. The sinogram is tomographically reconstructed to create an image of the source. See figure 2.f).

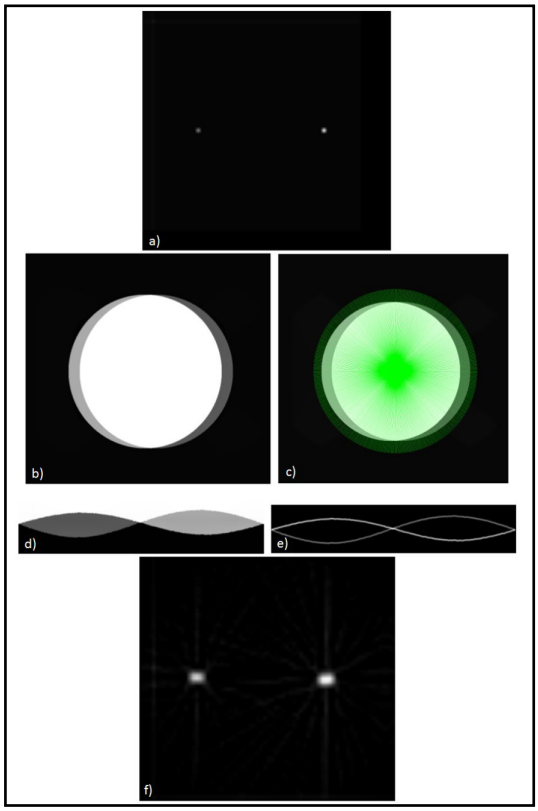

Figure 2. Depiction of the process of circular penumbra analysis, here using simulated data of two point sources. **a)** The simulated input data (source). **b)** The raw data circular penumbra image. **c)** The image is sliced radially. **d)** The slices are aligned side-by-side and unnecessary pixels are cropped out. **e)** The resulting sinogram. **f)** The reconstructed image of the source.

2.2 Mathematical Basis

Circular penumbra analysis is based on the three-plane experimental setup, and tomographic reconstruction of the raw CR data. Each plane has its own coordinate system. The source plane is double primed (''), the

object plane is single primed ('), and the detector plane is unprimed. See figure 1. To begin, a few distributions must be defined:

$\mu''(x''y''$: The distribution of the source in the source plane.
$A'(x',y')$: The distribution of the disk in the disk plane.
$\eta(x,y)$: The distribution of the penumbra image in the detector plane.

The two primed distributions must be transformed onto the detector plane using a magnification factor (or more accurately in the case of the TR camera, a "minification" factor), called M:

$$M = (p+q)/p \quad ...(1)$$

where p and q are defined on Figure 1. A distance r'' on the source plane can be transformed to the detector plane:

$$r = r''(M-1) \quad ...(2)$$

Similarly, a distance r' on the disk plane can be transformed to the detector plane:

$$r = r'M \quad ...(3)$$

The convolution of the source μ with the disk A in the detector plane, η, is defined as:

$$\eta(x,y) = \mu(x,y) \otimes A(x,y) \quad ...(4)$$

From this distribution, an image of the source is tomographically reconstructed. To simplify the math, a new set of axes is (x_r,y_r); for every slice of the penumbra, the x_r axis is parallel to the slice (along the $\hat{n}$ direction, at an angle θ from the x axis), and the y_r axis is tangent to the sharp edge of the disk. See figure 3.

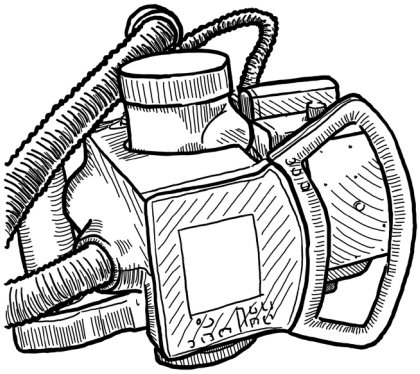

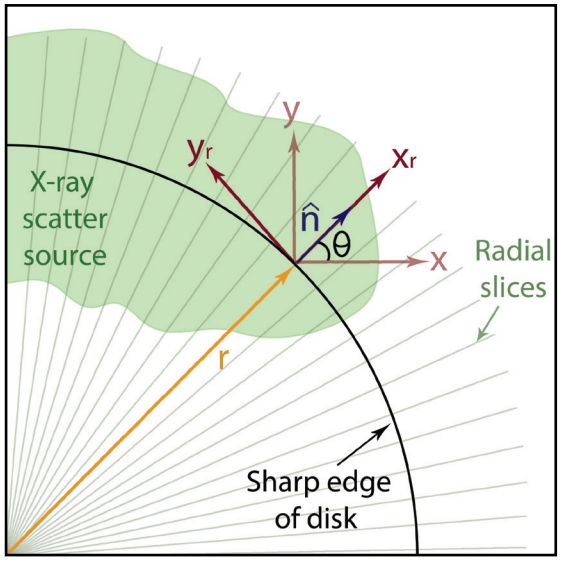

Figure 3. The (x_r,y_r) coordinate system simplifies the reconstruction process. The scatter source (projected onto the detector) is convolved with the disk (also projected onto the detector) to create the penumbra image.

Another measurement, r', must be considered, which points from the centre to the edge of the disk on the disk plane, and becomes r on the detector plane, per equation 3. With this value, the convolution can be written explicitly:

$$\eta(r) = \int A((r-r')\cdot\hat{n})\mu(r')d^2r' \quad ...(5)$$

Further, it can be rewritten in integral form, in terms of the (x_r,y_r) axes:

$$\eta_r(x_r,y_r)$$

$$= \int\int A(x_r - x_r')\mu_r(x_r',y_r')dx_r'dy_r'$$

$$= \int_{-\infty}^{x_r} dx_r' \int_{-\infty}^{+\infty} dy_r'\mu_r(x_r',y_r') \quad ...(6)$$

To obtain the projection along the x_r direction, the Radon transform is applied to equation 6:

$$\frac{dp_r}{dx_r} = \int_{-\infty}^{+\infty} \delta(x_r - x_r')\mu_r(x_r, y_r)dx_r'dy_r$$

$$= g(x_r, \theta) \quad ...(7)$$

Finally, the projection is transformed back to the *(x,y)* reference frame in which it is along a direction identified by the angle θ:

$$g(x_r, \theta)$$

$$= \int_{-\infty}^{+\infty}\int_{-\infty}^{+\infty} \delta(x_r - xcos\theta - ysin\theta)\mu(x,y)dxdy \quad ...(8)$$

Equation 8 shows that by taking the derivative of a slice perpendicular to the sharp edge at a particular angle θ, parametrized by the distance x_r, the projection of the original source distribution is obtained.

3. METHODS & RESULTS

3.1 Camera Fabrication

The camera (figure 4, left) had to be made of an x-ray-attenuating material, while taking into account manufacturing cost as well as weight, as it had to be portable. Steel (thickness 3/16" or 4.76 mm) was chosen as it best accommodated these limitations. The dimensions of the face were chosen so that the camera would be a close fit for the 18 cm x 24 cm CR plate. An aluminum frame was designed to hold the CR plate in place and to make its distance from the aperture adjustable (figure 4, right).

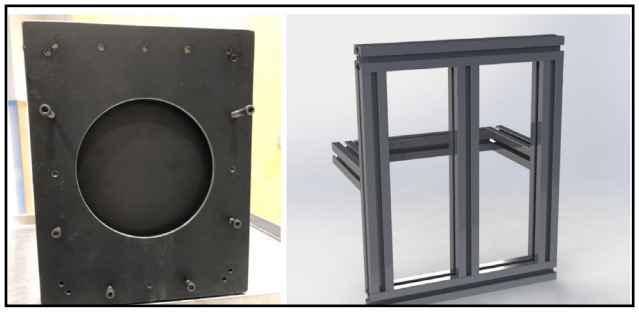

Figure 4. Left: The TR camera with a 15 cm diameter aperture, and the CR plate a few centimeters back from the aperture. The screws are in place in order to attenuate x-rays which could enter through holes that had been drilled into the camera face to accommodate a previous design. **Right**: The aluminum frame which supported the CR plate.

3.2 Simulated Data

In order to test the computer algorithm, a simulated input (two point sources, as in figure 2.a)) was convolved with a disk to produce a simulated penumbra image. The penumbra image was then processed using the algorithm, and a reconstruction faithful to the input (in terms of number, relative positions, and relative intensities) was returned (figure 2.f)). This confirmed that the algorithm was functional.

3.3 X-ray Point Sources

To provide proof of concept, data was collected from point sources using a radiographic tube at a distance of 300 cm, with 73 kVp and 0.4 mAs per exposure. Four points were exposed, with a different number of exposures per point, which created distinct relative intensities. The raw CR data was processed using the algorithm, and an image of the source was reconstructed and found to be accurate to the input. See figure 5.

Figure 5. Reconstruction of four point sources with varying intensities, created by applying a different number of exposures at each point.

3.4 X-ray Scatter

Later, the TR camera was set 1 m away from a fluoroscopy system with a torso phantom on the patient support table. The system was run until a DAP of 344 µGy m2 was reached (a dose within clinical levels). The resulting penumbra image was processed and an image of the x-ray scatter source was obtained. See figure 6.

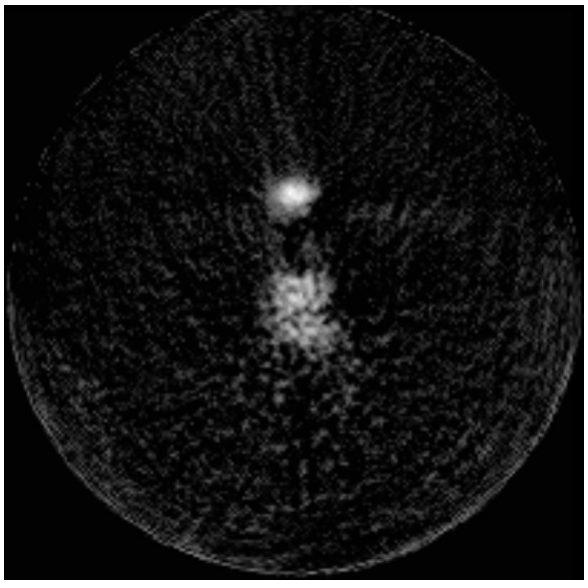

Figure 6. An x-ray scatter reconstruction, created using data collected from the TR camera being exposed to a fluoroscopy system with a torso phantom.

A pinhole camera was constructed similarly to the TR camera, with an aperture of 3 mm. It was exposed to x-ray scatter from the fluoroscopy system using the same experimental setup and was found to require eight times as much dose as the TR camera did in order to generate an image.

3.5 Overlaying Scatter with Photograph

In order to capture a photograph from the point of view of the TR camera, a box of the same dimensions as the TR camera was built to house a Raspberry Pi Camera Module v2. An opening was drilled in the front of this box, and a “chuck” to hold the digital camera was 3D printed. Prior to collecting data with the TR camera, the digital camera box was placed in the same location, and a photograph was taken. See figure 7.

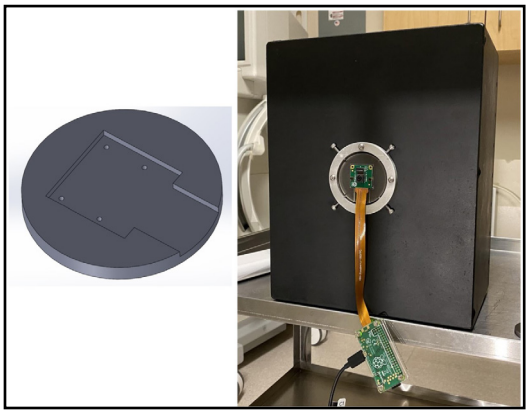

Figure 7. Left: A diagram of the 3D printed chuck which held the digital camera in place. **Right**: The digital camera box in place of the TR camera in order to collect a photograph from the same point of view. The chuck was held in place with 4 set screws.

To match the scatter reconstruction to the photograph, a scaling factor had to be determined. This was done using knowledge of the digital camera’s horizontal and vertical field of view (FOV), and the distances between the three planes. The focal length of the TR camera is the distance between the disk and the CR plate. The FOV of the

TR camera can be calculated with the following equation (note that the vertical and horizontal FOVs may not be the same, as the width and height of the reconstruction will often be unequal):

$$FOV = 2 \cdot arctan\left(\frac{width\ of\ height\ of\ reconstruction\ in\ px}{(px/cm\ on\ CR\ plate) \times 2 \times focal\ length}\right) \quad ...(9)$$

Knowing the FOV for both cameras (the vertical and horizontal FOVs of the digital camera were available from the manufacturer [Raspberry Pi]), the scaled width or height of the reconstruction can be found with the following equation:

$$reconstruction\ scaled\ width\ or\ height = \left(\frac{TR\ camera\ FOV}{digital\ camera\ FOV}\right) \times (photograph\ width\ or\ height) \quad ...(10)$$

The results of the overlay can be seen in figure 8.

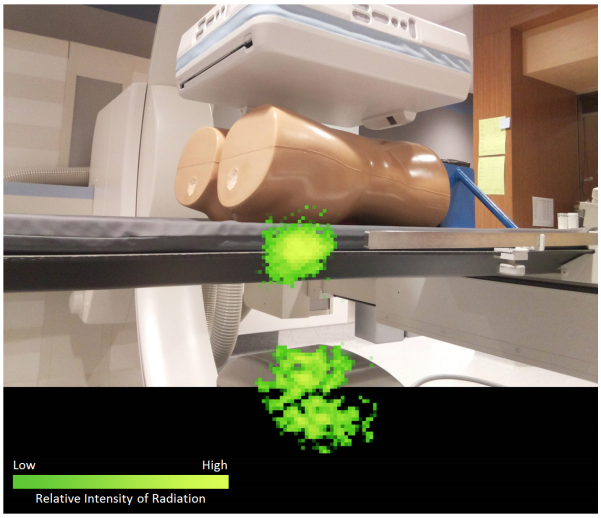

Figure 8. An x-ray scatter reconstruction (seen in figure 7) overlaid with the photograph of the scene. X-ray scatter is shown in green.

4. FUTURE INVESTIGATIONS

Future investigations will include the use of different types of phantoms. Of particular interest is a square prism acrylic phantom, which was used by Chida and colleagues, such that results could be better compared with Chida et al.'s results [Chida 2011]. Investigation into more accurate methods of measuring the focal length of the TR camera, and into more precise methods of mounting the digital camera (which has three degrees of freedom in which it could be inadvertently tilted, causing slight inaccuracy in the overlay image), would also be beneficial, in order to maximize accuracy of reconstruction-to-photograph scaling. Ultimately, it would be ideal to collect x-ray scatter data during clinical procedures.

REFERENCES

Chida, K., Takahashi, T., Ito, D., Shimura, H., Takeda, K., Zuguchi, M. (2011). Clarifying and visualizing sources of staff-received scattered radiation in interventional procedures. American Journal of Roentgenology, 197(5), 900-903. DOI:10.2214/AJR.10.6396

Di Domenico, G., Cardarelli, P., Contillo, A., Taibi, A., Gambaccini, M. (2016). X-ray focal spot reconstruction by circular penumbra analysis—Application to digital radiography systems. The International Journal of Medical Physics Research and Practice, 43(1), 294-302. http://dx.doi.org/10.1118/1.4938414.

Russo, P., Mettivier, G. (2011). Method for measuring the focal spot size of an x-ray tube using a coded aperture mask and a digital detector. The International Journal of Medical Physics Research and Practice, 38(4), 2099-2115. https://doi.org/10.1118/1.3567503.

Camera Module. Raspberry Pi. Retrieved March 2020, from https://www.raspberrypi.org/documentation/hardware/camera/.